Carbohydrate Polymers 79 (2010) 513–519

Contents lists available at ScienceDirect

Carbohydrate Polymers

journal homepage: www.elsevier.com/locate/carbpol

Isothermal crystallization kinetics of modified bamboo cellulose/PCL composites

Huaxi Liu [a,c], Yuanyuan Huang [a,c], Liang Yuan [a,c], Pingsheng He [a,c], Zhonghua Cai [a,c], Yiliang Shen [a], Youming Xu [b,c], Yan Yu [d], Hanguo Xiong [a,c,*]

[a] College of Food Science and Technology, Huazhong Agricultural University, Wuhan 430070, China
[b] College of Horticulture & Forestry Sciences, Huazhong Agricultural University, Wuhan 430070, China
[c] Research Institute of Comprehensive Utilization of Biomaterials, Huazhong Agricultural University, Wuhan 430070, China
[d] International Center for Bamboo and Rattan, Beijing 100102, China

ARTICLE INFO

Article history:
Received 29 June 2009
Received in revised form 25 August 2009
Accepted 27 August 2009
Available online 3 September 2009

Keywords:
Bamboo cellulose
PCL
Isothermal crystallization kinetics
DSC

ABSTRACT

For the purpose of utilizing bamboo cellulose and providing a theoretical basis, the isothermal crystallization kinetics of modified bamboo cellulose/poly(ε-caprolactone) (MBC/PCL) composites has been investigated by differential scanning calorimetry (DSC) at different crystallization temperature (T_c). The Avrami model was applied to describe the process of isothermal crystallization. According to Hoffman–Weeks theory, the values of the equilibrium melting point (T_m^0) increased with an increase in the content of MBC in the composites. The spherulite growth rate, the overall crystallization rate, the activation energy and folding-surface free energy (σ_e) of PCL/MBC composites are markedly affected by the presence of MBC. According to Avrami theory, MBC accelerates the crystallization of PCL in the composites. However, as compared to neat PCL, all the composites of PCL/MBC had the higher σ_e value. This indicates that there exist constraints on the mobility of the PCL chains in the interspherulitic regions due to the presence of MBC.

1. Introduction

Bamboos are the fastest growing woody plants in the world and contain a great deal of cellulose, hemicellulose and lignin. Bamboos are one of the strongest natural structural composite materials, with many distinguishing features. Due to the high water-repellent properties, the high flexibility, the high intensity, the low weight, the fast growing rate and the low purchasing costs, bamboo become more and more popular as a building material with many opportunities (Li, Zeng, Fu, & Zhou, 1995; Lugt, Dobbelsteen, & Janssen, 2006). In this paper, bamboo cellulose was made from waste bamboo scrap. In this way, the environment was protected and the waste was avoided.

Poly(ε-caprolactone) (PCL) is currently the most widely used commercial polymer. Because the social demands for degradable and biocompatible polymers is rapidly increasing, especially in the packaging sector where it is highly encouraged by environmental management policies (Flemming, 1998). PCL is synthetic, biodegradable polyester that is compatible with many types of polymers and it is one of the most promising biodegradable polymers currently available on the market. High cost and low melting temperature ($T_m \approx 60\,^{\circ}C$) are, however, the main limitations preventing the PCL widespread industrial use.

Recently, polymer composites materials have aroused much interest because these composites have unexpected properties, such as large increases in the thermal stability and mechanical strength. Many articles have been published on the synthesis and properties of composites of polymers materials (Chen & Wu, 2007; Day, Nawaby, & Liao, 2006; Ge, Ding, Sh, & Fu, 2009; Hua, Kai, & Inoue, 2007; Huda, Drzal, Mohanty, & Misra, 2007; Huda, Mohanty, Drzal, Schut, & Misra, 2005; Kalkar, Deshpande, & Kulkarni, 2009; Run, Song, Wang, Bai, & Jia, 2009; Wu & Chen, 2006; Zou, Tang, Fu, & Xiong, 2009). Among those composites, PCL composites have been reported many times and have gained much attention because of their novel properties, such as excellent thermal properties (Hua et al., 2007) and biodegradable (Chen & Wu, 2007).

As a means for overcoming the above-mentioned drawbacks of poly(ε-caprolactone) and avoiding waste bamboo, PCL is usually mixed with other low cost biodegradable polymers (De Kesel, Vander Wauven, & David, 1997; Nakayama et al., 1997). This method permits to alter the physical properties of one or both of the original components. Thus it may be anticipated that the miscible blending of bamboo cellulose with poly(ε-caprolactone) can improve their respective undesirable properties and exhibit a certain synergistic effect as well. The crystallization behavior of polymer is a basic problem in polymer physics. Especially the filler in a polymer will affect the crystallization behavior of the polymer-based composites very

* Corresponding author. Address: College of Food Science and Technology, Huazhong Agricultural University, Shizishan 1#, Wuhan 430070, China. Tel.: +86 2763215853; fax: +86 2787286608.

0144-8617/$ - see front matter © 2009 Elsevier Ltd. All rights reserved.
doi:10.1016/j.carbpol.2009.08.037

much (Kundu & Biswas, 2003). However, there is little information about the preparation and characterization of polymer/filler composites using the BC. The crystallization behavior of polymer is usually studied by DSC method. The crystallization process can proceed under either isothermal condition or non-isothermal conditions. Most frequently, the investigations are conducted under isothermal conditions because of the convenience of the theoretical treatment of the data. In this study, Effect of PCL on the isothermal crystallization kinetics and PCL/MBC composites were performed by the differential scanning calorimetry (DSC), and the parameters of the isothermal crystallization kinetics of PCL and PCL/MBC nanocomposites were also studied.

2. Experimental method

2.1. Materials

Bamboo cellulose (BC) with the size of 74 μm was provided by Research Institute of comprehensive utilization of Biomaterials, Huazhong Aggricultural University, China. Having been dried in 120 °C for 24 h, the surface of BC was modified by silane coupling agent (SG-Si900) (BC/SG-Si900 100/2 by weight), which was purchased from Nanjing Shuguang Chemical Co., before use. Meanwhile, PCL (M_n = 70,000) pellets were acquired from DAICEL CHEMICAL INDUSTRIES, LTD, Japan.

2.2. Preparation of MBC/PCL composites

The PCL and bamboo cellulose modified with silane coupling agent were mixed in a roller at 80–85 °C for 15–20 min. The resulting sheet was compressing molded at 100 °C into 1 mm thick sheet under a pressure of 9 MPa for 15 min, and kept at in room temperature. The ratios of modified bamboo cellulose/ poly(ε-caprolactone) (MBC/PCL) particle are (a) 0/100; (b) 20/100; (c) 40/100; (d) 60/100; (e) 80/100 and (f) 100/100 by weight, respectively.

2.3. Thermal analysis

Thermal analysis of the samples was carried out using a Nexus DSC 204F1 in nitrogen atmosphere. The temperature and melting enthalpy were calibrated with standard indium at each cooling rate in the measurement. Each sample was heated from 30 °C at a heating rate of 30 °C/min to 100 °C above the melting temperature. The sample was then held for 5 min to ensure complete melting and to eliminate residual anisotropy. Subsequently, each sample was rapidly cooled at the rate of 30 °C/min to the isothermal crystallization temperature (T_c) of interest 42, 41and 40 °C. The sample was held at desired isothermal temperature for the completion of the crystallization process till no change in the heat flow. The specimens were subsequently heated to 100 °C at a rate of 10 °C/min.

3. Results and discussion

The isothermal crystallization kinetics can be better visualized by evaluating the degree of crystalline conversion as a function of time at a constant temperature. The relative crystallinity at different crystallization time, X_t, can be calculated according to the equation:

$$X_t = \frac{\int_0^t (dH_c/dt)dt}{\int_0^{t\infty} (dH_c/dt)dt} \quad (1)$$

The isothermal thermograms of the PCL and MBC/PCL blends obtained by cooling a molten polymer to the crystallization temperature (T_c) are shown in Fig. 1. From Fig. 1, it was found that with increasing crystallization temperature the exothermic peaks shifted to a higher value. It can be see that the influence of crystallization temperature on crystallization is similar for both the PCL and MBC/PCL composites. Besides, adding MBC shortened the time to reach the crystallization half-time shown in Table 1, indicating an increase in crystallization rate. This implied that the MBC can act as a nucleating agent for the PCL matrix. The relative crystallinity (X_t) is obtained from the area of the exothermic peak of isothermal crystallization analysis in DSC, and it is plotted in Fig. 2. From Fig. 2 the relative crystallinity was decreasing at a certain crystallization time with an increase in T_c, which meant that the crystallization rate was decreasing. Besides, when the value of T_c is 40 °C, the rate of crystallization of the curve of c in Fig. 2 is faster than others.

3.1. Avrami theory

Generally, the theory of Avrami is used to analyze the increase of relative crystallinity with time:

$$1 - X_t = \exp(-Kt^n) \quad (2)$$

where K is the crystallization rate constant and n is Avrami exponent whose value depends on the mechanism of nucleation and on the form of crystal growth. X_t is the relative crystallinity of the polymers at different temperatures or time, t is the time taken during the crystallization process.

In order to deal conveniently with the operation, Eq. (1) usually rewritten as a double logarithmic form as follows:

$$\ln[-\ln(1 - X_t)] = \ln K + n \ln t \quad (3)$$

Accordingly, the Avrami exponent n and crystallization rate K can be obtained from the slope and intercept, respectively, in a plot of $\ln[-\ln(1 - X_t)]$ versus $\ln t$, as shown in Fig. 3. For the isothermal crystallization, a linear portion of about 30–70% (Liao, Yang, Yu, & Zhou, 2007) relative crystallinity was used to obtain n and k. Fig. 3 was the plots of $\ln[-\ln(1 - X_t)]$ versus $\ln t$ for isothermal crystallization of PCL/MBC. Meanwhile, the crystallization half-time $t_{1/2}$ is the time at which the extent of crystallization is 50%, which is defined as $t_{1/2} = (\ln 2/K)^{1/n}$. The Avrami exponent n, the crystallization rate constant K, and the crystallization half-time $t_{1/2}$ at different crystallization temperatures are listed in Table 1.

In the Avrami expression, the Avrami exponent n provides qualitative information on the nature of nucleation and the growth processes. An Avrami exponent n with value close to three is attributed to three-dimensional crystal growth (spherical structure) resulting from instantaneous athermal nucleation process. On the other hand, an n value between two and three represents non three-dimensional truncated spherical structures resulting from instantaneous nucleation, controlled by diffusion process. The non-integral n values indicate the presence of the combination of thermal and athermal mixed nucleation and mechanisms (Kalkar et al., 2009).

From Table 1, it was found that with increasing crystallization temperature the exponent n was increasing in most of samples, and moreover, it can be observed that the exponent n is found to range from 1.81 to 2.70 (the most of n value between two and three). This indicates to gradual growth of two-dimensional morphology to a spherical three-dimensional morphology with a combination of thermal and athermal nucleation.

The values of K, which is related to nucleation rate and growth processes, decreased with an increase in T_c in the cases of a, b, c, d and f (Table 1), which meant that the crystallization rate was decreasing. The incorporation of MBC significantly increased the crystallization kinetic constant K, suggesting that MBC can act as effective nucleating agents and accelerate the crystallization of PCL in the composites. Generally, $t_{1/2}$ is used to characterize the crystallization rate, and the longer the $t_{1/2}$, the slower the crystallization

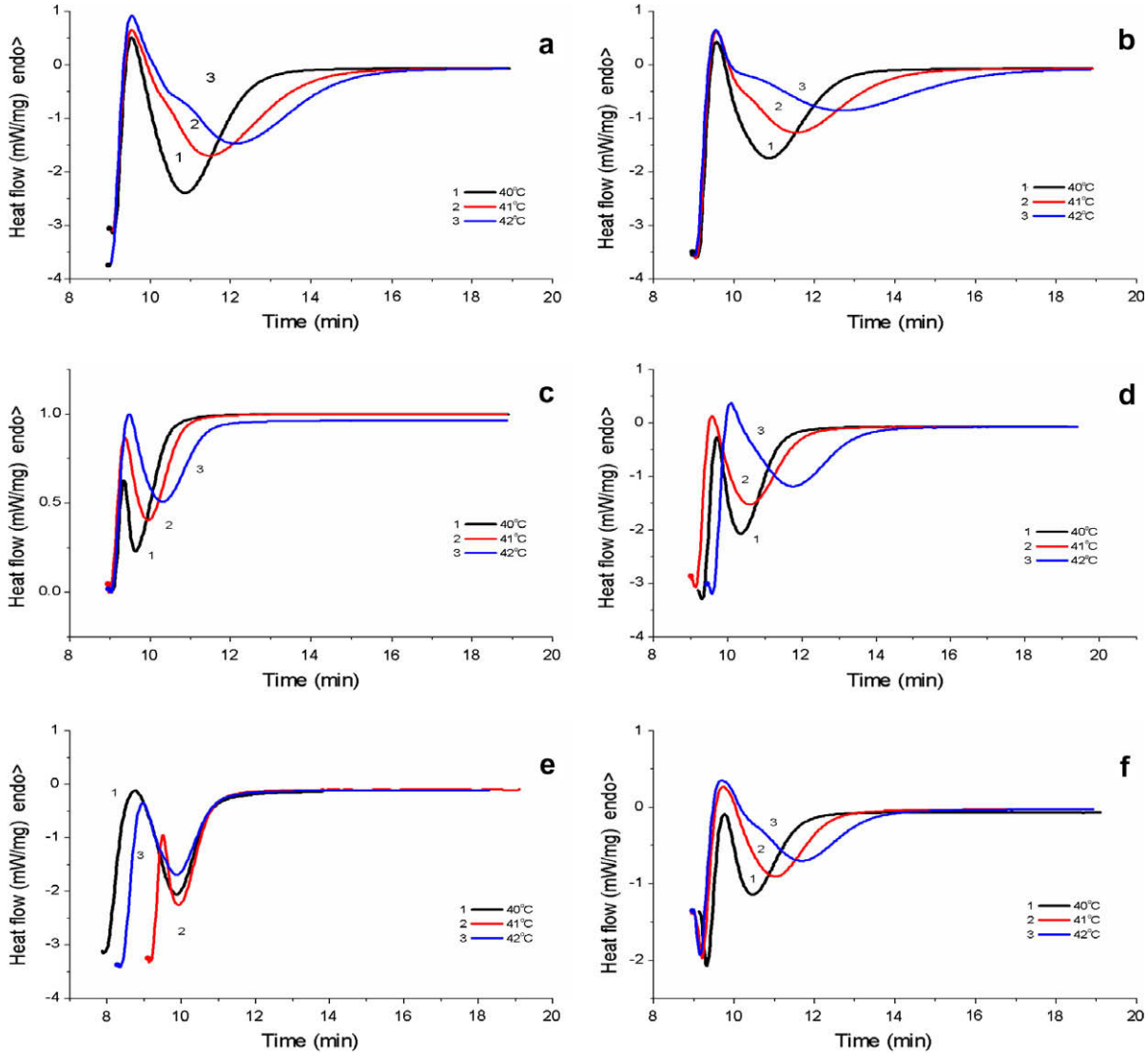

Fig. 1. The DSC traces of samples isothermally crystallized at the specified temperature: (a) PCL:MBC = 100:0; (b) PCL:MBC = 100:20; (c) PCL:MBC = 100:40; (d) PCL:MBC = 100:60; (e) PCL:MBC = 100:80; (f) PCL:MBC = 100:100 (by weight).

Table 1
Avrami kinetic parameters from the Avrami equation and value of ΔE for the isothermal crystallization of samples.

Samples	T_c (°C)	$t_{1/2}$ (min)	n	K (min^{-1})	ΔE (kJ/mol)
PCL/MBC	40	1.15976	2.2	0.50	−226.3
(100/0 w/w)	41	1.73617	2.2	0.21	
	42	2.02740	2.3	0.14	
PCL/MBC	40	1.10258	2.1	0.57	−366.6
(100/20 w/w)	41	1.64185	2.3	0.22	
	42	2.77010	2.5	0.06	
PCL/MBC	40	0.35297	1.8	4.57	−253.9
(100/40 w/w)	41	0.45210	2.1	3.55	
	42	0.67223	2.1	1.58	
PCL/MBC	40	0.61819	2.0	1.81	−327.8
(100/60 w/w)	41	0.93507	2.1	0.80	
	42	1.40568	2.3	0.32	
PCL/MBC	40	0.94154	2.7	0.82	−464.8
(100/80 w/w)	41	0.42896	1.9	3.49	
	42	0.78160	2.3	1.22	
PCL/MBC	40	0.64185	2.0	1.67	−363.0
(100/100 w/w)	41	1.02581	2.2	0.66	
	42	1.59376	2.3	0.24	

rate. In most of samples (a, b, c, d and f), $t_{1/2}$ increases with an increase in T_c. The $t_{1/2}$ values of the composites are lower than those of neat PCL. This implies that MBC accelerates the crystallization of PCL in the composites, which is in accordance with the above result.

3.2. Isothermal crystallization activation energy (Ge et al., 2009; Run et al., 2009)

In the isothermal crystallization process, activation energy was obtained from the slopes of the plots of $(1/n)\ln K$ versus $1/RT_c$ by the Arrhenius equation as:

$$\frac{1}{n}\ln K = \ln(K_0) - \frac{\Delta E_a}{RT_c} \tag{4}$$

where K, crystallization rate constant; T_c, crystallization temperature; K_0, pre-exponential constant; R, gas constant. ΔE_a, total apparent activation energy. $\Delta E_a = \Delta F + \Delta\varphi$, where, ΔF transformation activation energy or an activation energy of a unit crystallite crossing through the liquid solid interface of a polymer; $\Delta\varphi$ nucleation

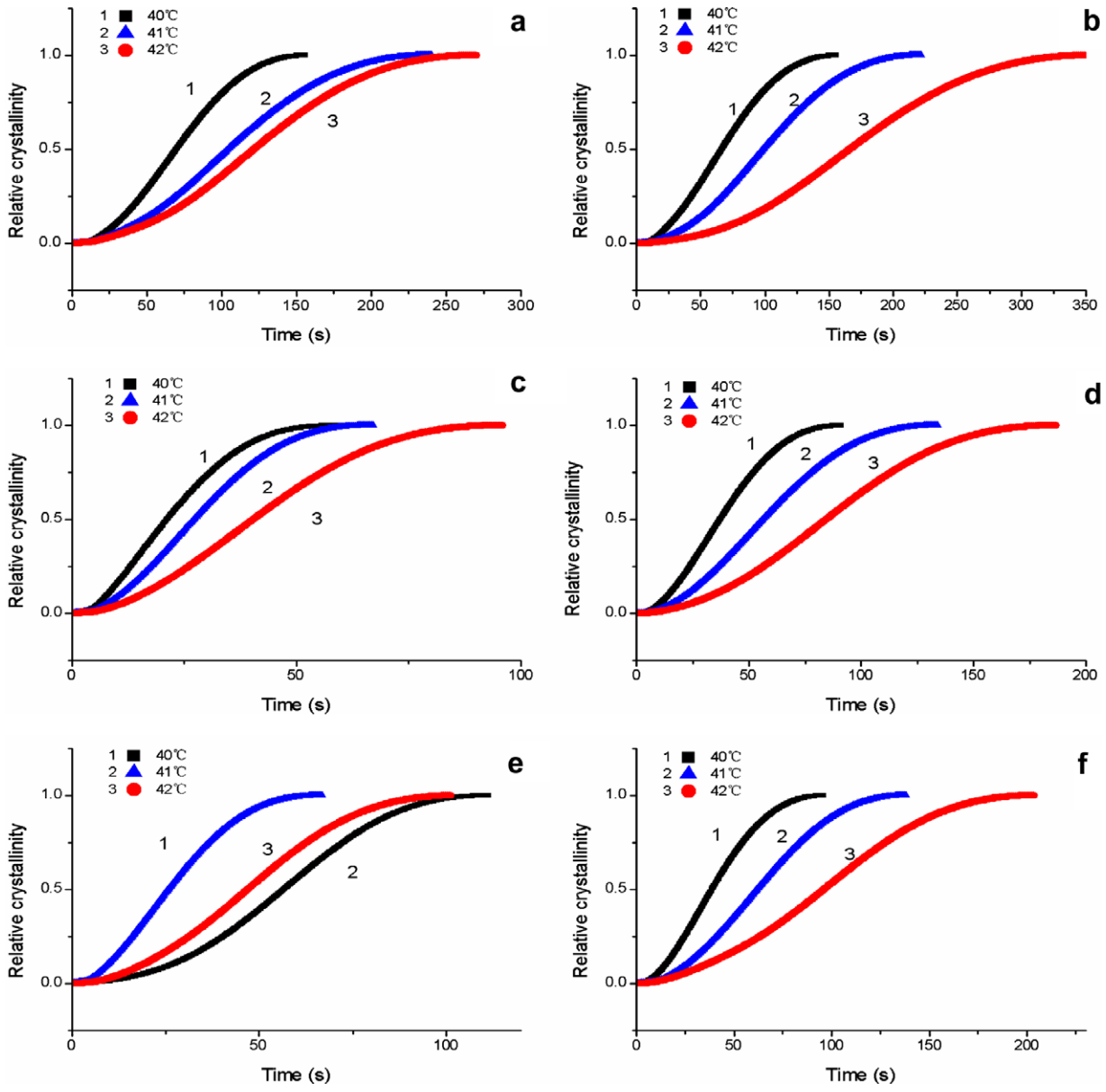

Fig. 2. Plots of X_t versus t for the isothermal crystallization of samples at the specified temperature: (a) PCL:MBC = 100:0; (b) PCL:MBC = 100:20; (c) PCL:MBC = 100:40; (d) PCL:MBC = 100:60; (e) PCL:MBC = 100:80; (f) PCL:MBC = 100:100 (by weight).

activation energy or the activation energy for forming critical sized nuclei at crystallization temperature T_c. At high crystallization temperature from melt, the nucleation activation energy $\Delta\varphi/(RT_c)$ dominates at very low supercool degree, the item of $\Delta F/(RT_c)$ in the multinomial expression is omitted. Thus, $\Delta\varphi$ approximately expressed the total activation energy ΔE_a.

Plots of $1/n$ ($\ln k$) against $1/RT_c$ for PCL and PCL/MBC nanocomposites are shown in Fig. 4, and The curves of $(1/n)\ln K$ versus $1/RT_c$ were plotted from the data listed in Table 1. From the Table 1, it can be see that as compared to neat PCL, the composites of PCL/MBC had a lower ΔE_a value. This result suggests that the addition of MBC into PCL matrix can induce the heterogeneous nucleation and increase the crystallization ability of PCL during the crystallization processes.

3.3. Equilibrium melting point (T_m^0)

To carry on with the quantitative analysis of crystallization behavior, especially to investigate the temperature dependence of crystallization rate, it is necessary to determine the equilibrium melting point as accurately as possible. The reliable estimation of the equilibrium melting point can be made by careful DSC studies. According to the Hoffman–Weeks theory, the equilibrium melting point may be deduced by plotting the observed apparent melting temperature (T_m) against the crystallization temperature (T_c). The equilibrium melting point is obtained by an extrapolation of the resulting straight line to intersect the line $T_m = T_c$. The values of T_m^0 are listed in Table 2. As is shown in the table, the values of T_m^0 increase with an increase in content of MBC in the composites.

3.4. Hoffman and Lauritzen theory

From the isothermal crystallization, the growth rate of crystallization, G, defined as $G = 1/(t_{1/2})$, is obtained from the endotherm morphology of DSC analysis. The growth rate of crystallization can be expressed as follows according to the Hoffman and Lauritzen theory:

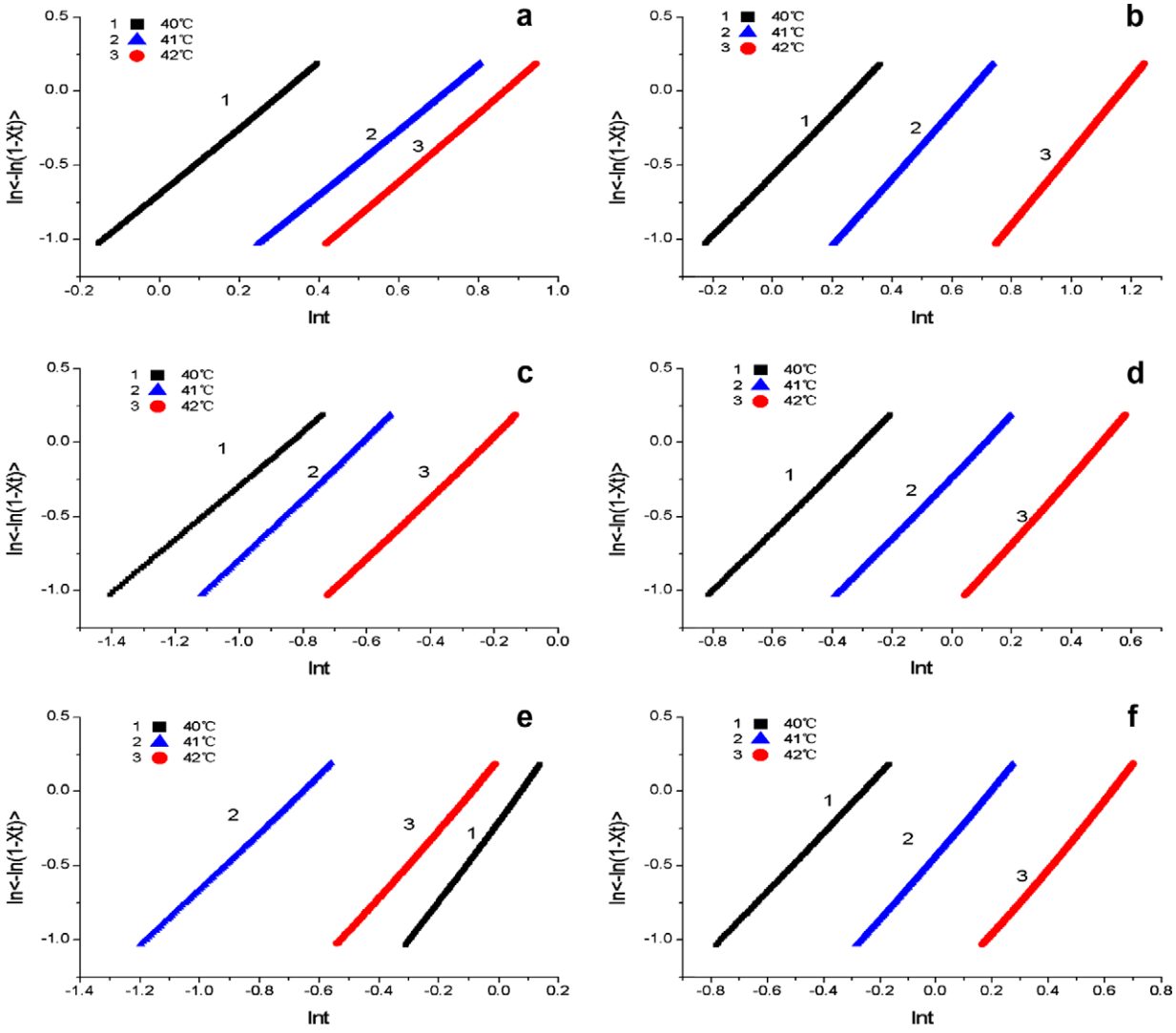

Fig. 3. Plots of $\ln[-\ln(1-X_t)]$ versus $\ln t$ for the isothermal crystallization of samples at the specified temperature: (a) PCL:MBC = 100:0; (b) PCL:MBC = 100:20; (c) PCL:MBC = 100:40; (d) PCL:MBC = 100:60; (e) PCL:MBC = 100:80; (f) PCL:MBC = 100:100 (by weight).

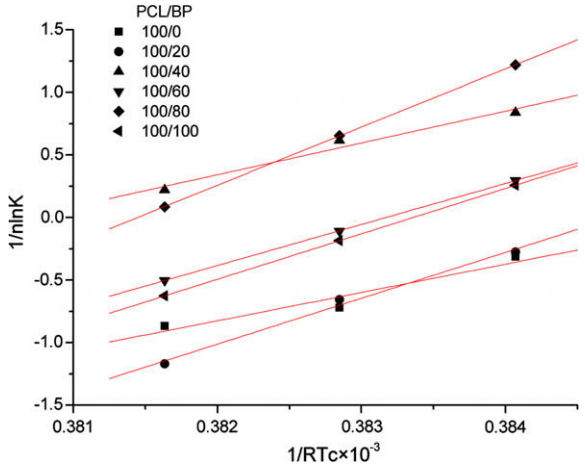

Fig. 4. Arrhenius plots of $1/n$ (ln k) versus $1/RT_c$ for PCL and PCL/MBC composites.

$$G = G_0 \exp\left[-\frac{U^*}{R(T_c - T_\infty)}\right] \exp\left[-\frac{K_g}{T_c \Delta T_f}\right] \quad (5)$$

where G_0 is a pre-exponential term, ΔT is equal to $T_m^0 - T_c$, R is the universal gas constant, U^* is the diffusional activation energy for the transport of crystallizable segments at the liquid–solid interface, and the recommended values $U^* = 17300$ J/mol (Meng, Wen, Li, & Tang, 2006). T_c is the crystallization temperature, and T_∞ is the hypothetical temperature below which viscous flow ceases. Meanwhile, Hoffman et al. found $T_\infty = T_g - 30$ K; $f = 2T_c/(T_m^0 + T_c)$. It is most convenient to rearrange Eq. (4) as follows:

$$In\,G + U^*/[R(T_c - T_\infty)] = \ln G_0 - K_g/(T_c \Delta T_f) \quad (6)$$

According to Eq. (4), a plot of $\ln G + U^*/[R(T_c - T_\infty)]$ against $1/(T_c \Delta T_f)$ should yield a straight line with an intercept $\ln G_0$ and a slope $-K_g$. The nucleation constant K_g is listed in Table 2. The K_g for the MBC/PCL composites are higher than those for pure PCL.

Table 2
Values of T_m^0, K_g, G_0, q and σ_e for PCL and PCL/MBC composites.

PCL/MBC (w/w)	T_m^0 (K)	K_g (K^2)	G_0 ($\times 10^5$)	$\sigma_e \times 10^3$ (J/m^2)	q (kJ/mol)
100/00	332.8	35080	4.6	37.91	8.5
100/20	333.6	61752	302.2	66.58	14.9
100/40	334.3	47450	74.9	51.06	11.4
100/60	334.7	62077	337.3	66.71	14.9
100/80	335.2	89181	40218.2	95.69	21.4
100/100	335.4	73555	1307.8	78.87	17.7

The nucleation constant K_g contains contributions from the surface free energies, and it can be obtained from Eq. (5):

$$K_g = \frac{rb_0\sigma\sigma_e T_m^0}{k\Delta H_m^0} \quad (7)$$

where σ and σ_e are the lateral and surface free energies of the growing crystal, respectively, the value of σ is 7.14×10^{-3} J/m^2, the recommended values $\Delta H_m^0 = 1.63 \times 10^8$ J/m^2, and b_0 is the distance between two adjacent fold planes, taken to be the perpendicular separation of planes. This is 4.38×10^{-10} m (Meng et al., 2006). k is the Boltzmann constant, and r is a variable that considers the crystallization regime and assumes the value 4 for the regimes I and III, and the value 2 for the regime II.

To judge whether the crystal growth occurs in regime I or II, the Z test of Lauritzen is available. The Z value is defined as:

$$Z \approx 10^3 (L/2b_0)^2 \exp\,[-X/(T_c\Delta T)] \quad (8)$$

where L is the crystalline substrate length corresponding to an effective lamellar width. Regime I kinetics is obeyed if substitution of $X = K_g$ in the above equation leads to $Z < 0.01$; if Eq. 8 with $X = 2\,K_g$ results in $Z > 1$, then regime II growth is indicated. Actually, however, the regime is determined by deciding whether the range of L values calculated in each case is reasonable (Kalkar et al., 2009). Testing the K_g data in Table 3 for conformity to regime I led to the limits of L to be <0.048 nm for PCL and <0.10–1.77 nm for the four series of blends, all unrealistically small. Testing for regime II produced more reasonable L values of >15 nm for PCL and >73–37677 nm for the blends. Accordingly, it can be taken that the crystallization of PCL in all the samples proceeded according to regime II.

σ was often estimated by Thomas–Stavely empirical equation as follows:

$$\sigma = 0.1 b_o(\Delta H_m^0) \quad (9)$$

For PCL, σ is estimated as 0.007139 J/m^2 by using a data of $\Delta H_m^0 = 1.63 \times 10^8$. The K_g values are used to calculate the folding-surface free energy according to Eq. (5), and the result of the calculation of the folding-surface free energy σ_e is summarized in Table 2. As compared to neat PCL, all the composites of PCL/MBC had the higher σ_e value. As σ_e is strongly correlated with the work of chain folding $q = 2A_0\sigma_e$ Where A_0 is the cross sectional area of polymer, the value of A_0 is 0.186×10^{-18} m^2) (Meng et al., 2006), which is further understood in terms of bending of polymer chain back upon itself, the higher σ_e value in composites indicates that there exist constraints on the mobility of the PCL chains in the interspherulitic regions due to the presence of MBC.

4. Conclusions

A systematic study of the isothermal crystallization kinetics of the neat PCL and the MBC/PCL composites has been performed by DSC.

Table 3
Maximum substrate length (L in μm) required for the crystallization to fall in regime II, using Lauritzen Z test.

PCL/MBC (w/w)	Isothermal crystallization temperature (°C)		
	40	41	42
100/00	0.0083	0.0111	0.0153
100/20	0.4280	0.6806	1.1382
100/40	0.0363	0.0506	0.0731
100/60	0.2732	0.4144	0.6561
100/80	11.3509	20.0961	37.6775
100/100	1.0415	1.6490	2.7326

As compared to the crystallization process of neat PCL, adding MBC shortened the time to reach the crystallization half-time. This implied that the MBC can act as a nucleating agent for the PCL matrix. With increasing crystallization temperature the exponent n was increasing in most of samples, and moreover, it can be observed that the exponent n is found to range from 1.81 to 2.70 (the most of n value between two and three). This indicates to gradual growth of two-dimensional morphology to a spherical three-dimensional morphology with a combination of thermal and athermal nucleation. The incorporation of MBC significantly increased the crystallization kinetic constant K, suggesting that MBC can act as effective nucleating agents and accelerate the crystallization of PCL in the composites. As compared to neat PCL, the composites of PCL/MBC had a lower ΔE_a value. This result suggests that the addition of MBC into PCL matrix can induce the heterogeneous nucleation and increase the crystallization ability of PCL during the crystallization processes. According to the Z test, the crystallization of PCL in all the samples proceeded according to regime II. As compared to neat PCL, all the composites of PCL/MBC had the higher σ_e value. This indicates that there exist constraints on the mobility of the PCL chains in the interspherulitic regions due to the presence of MBC.

Acknowledgments

We acknowledge the financial assistance support for this work from the National Eleventh Five-Year plan Foundation of China (No. 2008BADA9B01) and the National Natural Science Foundation of China (20976066).

References

Chen, E. C., & Wu, T. M. (2007). Isothermal crystallization kinetics and thermal behavior of poly(epsilon-caprolactone)/multi-walled carbon nanotube composites. *Polymer Degradation and Stability, 92*(6), 1009–1015.

Day, M., Nawaby, A. V., & Liao, X. (2006). A DSC study of the crystallization behaviour of polylactic acid and its nanocomposites. *Journal of Thermal Analysis and Calorimetry, 86*(3), 623–629.

De Kesel, C., Vander Wauven, C., & David, C. (1997). Biodegradation of polycaprolactone and its blends with poly(vinylalcohol) by micro-organisms from a compost of house-hold refuse. *Polymer Degradation and Stability, 55*, 107–113.

Flemming, H. C. (1998). Relevance of biofilms for the biodeterioration of surfaces of polymeric materials. *Polymer Degradation and Stability, 59*, 309–315.

Ge, C. H., Ding, P., Sh, L. Y., & Fu, J. F. (2009). Isothermal crystallization kinetics and melting behavior of poly(ethylene terephthalate)/barite nanocomposites. *Journal of Polymer Science Part B-Polymer Physics, 47*(7), 655–668.

Hua, L., Kai, W. H., & Inoue, Y. (2007). Crystallization Behavior of poly(epsilon-caprolactone)/graphite oxide composites. *Journal of Applied Polymer Science, 106*(6), 4225–4232.

Huda, M. S., Drzal, L. T., Mohanty, A. K., & Misra, M. (2007). The effect of silane treated- and untreated-talc on the mechanical and physico-mechanical properties of poly(lactic acid)/newspaper fibers/talc hybrid composites. *Composites Part B-Engineering, 38*(3), 367–379.

Huda, M. S., Mohanty, A. K., Drzal, L. T., Schut, E., & Misra, M. (2005). "Green" composites from recycled cellulose and poly(lactic acid): Physico-mechanical and morphological properties evaluation. *Journal of Materials Science, 40*(16), 4221–4229.

Kalkar, A. K., Deshpande, V. D., & Kulkarni, M. J. (2009). Isothermal crystallization kinetics of poly(phenylene sulfide)/TLCP composites. *Polymer Engineering and Science, 49*(2), 397–417.

Kundu, P. P., & Biswas, J. (2003). Influence of film preparation procedures on the crystallinity, morphology and mechanical properties of LLDPE films. *European Polymer Journal, 39*, 1585–1593.

Li, S. H., Zeng, Q. Y., Fu, S. Y., & Zhou, B. L. (1995). Biomimicry of bamboo bast fiber with engineering composite materials. *Materials Science and Engineering, 3*, 125–130.

Liao, R. G., Yang, B., Yu, W., & Zhou, C. X. (2007). Isothermal cold crystallization kinetics of polylactide/nucleating agents. *Journal of Applied Polymer Science, 104*(1), 310–317.

Lugt, P. v. d., Dobbelsteen, A. A. J. F. v. d., & Janssen, J. J. A. (2006). An environmental, economic and practical assessment of bamboo as a building material for supporting structures. *Construction and Building Materials, 20*, 648–656.

Meng, Y. F., Wen, H. Y., Li, H. F., & Tang, Y. J. (2006). Investigation on isothermal and non-isothermalcrystallization kinetics of Poly(ε-caprolactone). *Chemical Journal of Chinese Universities, 11*, 2198–2203.

Nakayama, A., Kawasaki, N., Maeda, Y., Arvanitoyannis, I., Ariba, S., & Yamamoto, N. (1997). Study of biodegradability of poly(D-valerolactone-co-L-lactide)s. *Journal of Applied Polymer Science, 66*, 741–748.

Run, M. T., Song, H. Z., Wang, S. J., Bai, L. B., & Jia, Y. H. (2009). Crystal morphology, melting behaviors and isothermal crystallization kinetics of SCF/PTT composites. *Polymer Composites, 30*(1), 87–94.

Wu, T. M., & Chen, E. C. (2006). Isothermal and nonisothermal crystallization kinetics of poly(epsilon-caprolactone)/multi-walled carbon nanotube composites. *Polymer Engineering and Science, 46*(9), 1309–1317.

Zou, P., Tang, S. W., Fu, Z. Z., & Xiong, H. G. (2009). Isothermal and non-isothermal crystallization kinetics of modified rape straw flour/high-density polyethylene composites. *International Journal of Thermal Sciences, 48*(4), 837–846.